FISEVIER

Contents lists available at ScienceDirect

Separation and Purification Technology

journal homepage: www.elsevier.com/locate/seppur



Improvement in flux and antifouling properties of PVC ultrafiltration membranes by incorporation of zinc oxide (ZnO) nanoparticles



Hesamoddin Rabiee ^a, Vahid Vatanpour ^{b,*}, Mohammad Hossein Davood Abadi Farahani ^a, Hamed Zarrabi ^a

ARTICLE INFO

Article history:
Received 19 July 2015
Received in revised form 3 October 2015
Accepted 6 October 2015
Available online 23 October 2015

Keywords: Emulsion polyvinyl chloride ZnO Nanocomposite membrane Ultrafiltration Antifouling

ABSTRACT

In this study, modification of polyvinyl chloride (PVC) ultrafiltration membranes with zinc oxide (ZnO) nanoparticle addition was taken into consideration. The ZnO at five different weights was added to the polymeric solution, and the membranes were fabricated by the phase inversion method using water as a nonsolvent and PEG 6 kDa as a pore former additive. The results showed that the pure water flux of the modified membranes increased up to 3 wt% ZnO addition, which was the optimized amount of the nanoparticle addition in this study. Also, at 3 wt% ZnO addition, flux recovery ratio reached from 69% to above 90%, indicated that the nanocomposite membranes were less susceptible to be fouled. BSA rejection of the membranes also enhanced up to 97% by 3 wt% ZnO addition. The membranes were further characterized by SEM images and remarkable changes in their morphologies were observed, and they became more porous with higher interconnectivity between the pores. Furthermore, EDAX analysis was applied to study ZnO dispersion in the membrane structure and except for 4 wt% ZnO addition which particles aggregation was noticeable, ZnO was dispersed finely in the membrane structure. In addition, the modified membranes had higher hydrophilicity and lower contact angle that was effective to obtain higher water flux.

© 2015 Elsevier B.V. All rights reserved.

1. Introduction

During the last decades, using membrane separation processes for different applications like gas separation [1], protein concentration [2] and water treatment [3] has been quite remarkable. These processes show interesting separation efficiency, technical benefits and reasonable operating costs. For the case of water and wastewater treatments, these types of separation and purification seem more under attention due to serious concerns about drinking water shortage and methods of resolving within the last decades and future [4]. In this regard, different types of membranes have been used for the case of water treatment, such as reverse osmosis (RO) [5], forward osmosis (FO) [6], filtration membranes [7–9] and membrane bioreactor (MBR) [10]. Among these processes, water purification with filtration membranes and its modification has been always a hot topic in the membrane science applications. The membranes for this purpose are usually prepared via nonsolvent induced phase separation (NIPS) or thermally introduced phase separation (TIPS), of which NIPS is rather more considered due to more flexibility and ease of the process [11,12].

The filtration membranes are normally made of some polymeric highly used materials like: polyvinylidene fluoride (PVDF) [13], polysulfone (PSf) [14], polyethersulfone (PES) [15], cellulose acetate (CA) [16], polyacrylonitrile (PAN) [17,18], polyvinyl chloride (PVC) [7,19] and polyether imide (PEI) [20]. Among these materials, PVC seems to be a suitable choice for membrane preparation because of excellent chemical, thermal and mechanical properties and also reasonable cost in comparison with the others. Recently, our group [7] have prepared emulsion PVC UF membranes via the phase separation using N-methyl-pyrrolidinone (NMP) as a solvent and investigated addition of polyethylene glycol (PEG 6 kDa) in the membrane structure. The results showed that the membranes fabricated with PVC possess good water flux and interesting flux recovery and rejection properties. Moreover, as PVC can be dissolved in various industrial solvents like N,N dimethyl acetamide (DMAc) [21-23], NMP [7], tetrahydrofuran (THF) [24] and dimethylformamide (DMF) [25], it is quite flexible for industrial applications and units.

Performance of ultrafiltration PVC membranes with addition of different additives have been studied by Mei et al. [26], and they reported that existence of PVP additives in polymeric solution leads to faster instantaneous demixing and solvent–nonsolvent exchange during membrane preparation and consequently, more

^a Department of Chemical and Petroleum Engineering, Sharif University of Technology, PO Box 11155-9465, Azadi Avenue, Tehran, Iran

^b Faculty of Chemistry, Kharazmi University, Tehran, Iran

^{*} Corresponding author.

E-mail address: vahidvatanpour@khu.ac.ir (V. Vatanpour).

fingerlike porous structure [26]. Addition of Pluronic F127 has also led to better antifouling properties of the PVC membranes; however, pure water flux through the membranes reduced, which is due to reduction in surface pore size and overall porosity [22]. These methods and preparation situations were considered to modify membrane morphology and improved membrane separation ability along with higher water flux. As, commonly used polymeric materials are usually very hydrophobic, they can be fouled easily in the presence of hydrophobic microorganisms and proteins, thereby their efficiency changes [27]. Therefore, the other methods of membrane modification have been taken into consideration during the last decades, as well.

Membrane preparation from mixture systems with two polymers with different properties has been considered either [23,28–30]. This is an easy way to get advantages of both polymers and especially reduce membrane's hydrophobicity by blending with a less hydrophobic one.

Another method of membrane modification which has been fairly successful to fabricate membranes with better antifouling properties is incorporation of the nanoparticles. In this regards, various types of particles such as: alumina (Al₂O₃) [31], silica (SiO_2) [32], titanium oxide (TiO_2) [33–35], boehmite [36], graphene oxide [37], carbon nanotube [38,39], ZrO₂ [40,41] and zinc oxide (ZnO) [42–45] were used in the preparation of mixed matrix membranes. Addition of TiO₂ nanoparticles into PVC structure has been recently studied by our group, and the results showed that TiO₂ addition up to 2 wt% caused to higher water flux, more recovery ratio and better antifouling properties, which were mainly due to increment of membrane hydrophilicity and more fingerlike pores across the membranes [8]. Likewise, for the case of TiO₂ addition into PES UF membranes, lower fouling ratio and higher water flux was observed [35]. It is also found that due to inorganic nature of the nanoparticles, their addition led to better thermal stability and mechanical strength of the fabricated membranes. TiO2 nanoparticles in various types have been studied for membrane modification, and the research carried out in this respect shows that TiO₂-P25 nanoparticles has the least tendency to aggregate, and they are more desirable to enhance antifouling properties of filtration membranes [33]. Maximus et al. precisely inspected incorporation of Al₂O₃ and ZrO₂ nanoparticles into PES UF membranes and observed that the both particle-modified membranes had higher porosity, better antifouling properties and be more permeable for water [31,40,46]. Vatanpour et al. have lately studied the effect of amine modified carbon nanotubes on PES flat sheet nanofiltration membranes and observed higher surface hydrophilicity and water flux, compared to the bare one [39].

In comparison with TiO₂, SiO₂ and Al₂O₃, less attention has been paid to utilize ZnO for membrane modification. Shen et al. prepared ZnO-modified PES membranes with using PEG400 as the pore former additive [42]. They showed that addition of ZnO in PES structure led to improved hydrophilicity, porosity and enhancement in water flux, flux recovery and antifouling ability of the membranes. Zhao et al. have recently studied the effect of ZnO nanoparticles on PES membranes either, and reported about 110-220% increment in water permeation, and also observed reduction in irreversible resistance of the membranes [45]. Liang et al. modified internal surface of the PVDF membranes with ZnO addition up to 27% of polymer weight [44]. Their result in recovery was excellent, and all the modified membranes were able to maintain the constant initial fluxes in multi-cycle filtration (100% recovery) while for the bare membrane, they reported 78% recovery. They related this outstanding promotion to increment of inner surface hydrophilicity. Additionally, they observed twice water flux compared to the bare membrane for the modified membranes. Similar results were also reported for ZnO addition to PSf membranes indicated highly enhanced water flux and better thermal stability [43].

As recently, the incorporation of TiO₂ nanoparticles in PVC membranes has been widely studied by our group and to the best of our knowledge, effects of ZnO addition of PVC UF membranes have not been worked on yet, therefore, the current research concentrates on PVC/ZnO UF membranes. The membranes are prepared via nonsolvent induced phase inversion with NMP as the solvent and water as the nonsolvent. ZnO at different loadings was added to membrane structure and pure water flux, BSA permeation and flux recovery ratio were measured and calculated. The membranes' morphology was studied by SEM images, and their hydrophilicity was studied using contact angle results.

2. Experimental

2.1. Materials

Emulsion polyvinyl chloride (EPVC) was supplied from Arvand Petrochemical Co., Iran. 1-Methyl 2-pyrrolidone (NMP) as the polymer solvent and polyethylene glycol (PEG) with molecular weight of 6 kDa were purchased from Merck, Germany. ZnO nanoparticles were purchased from US Nano with particle size of 20–30 nm. Bovine serum albumin (BSA) was used as a foulant and was bought from Sigma.

2.2. PVC/ZnO UF membrane preparation

The PVC/ZnO UF flat sheet asymmetric membranes were prepared via the immersion precipitation phase inversion method which has been explained elsewhere [8]. Briefly, at the first step, the specific amounts of ZnO were mixed and dispersed in NMP and sonicated for around 2 h to obtain homogenous suspensions. Based on the literature ZnO at 5 different percentages (0.3, 1, 2, 3 and 4 wt%) was added to membrane structure [43,44]. After that, PEG 6 kDa were added to the mixtures, and stirred to dissolve. The amount of PEG in the final polymeric solution was 4 wt%. The PEG dissolved firstly because it improves the dispersion of the ZnO nanoparticles. Subsequently, 10 wt% of PVC was added to the suspensions and stirred for 24 h to be dissolved completely. Then, the remaining amounts of polymer were added to have polymeric solutions with 15 wt% PVC. After having complete homogenous PVC/PEG/NMP/ZnO mixtures, the solutions were sonicated for 1 h to remove any possible air bubbles. After that, the membranes were casted on a glass plate using of a 150 µm casting knife at room temperature. Then promptly, the coated glass was immersed in a nonsolvent bath, which is full of water at room temperature. After 15 min, the prepared samples were placed in another bath full of fresh water to be sure that the solvent and the additives were leached. The compositions of the fabricated samples are shown in Table 1.

2.3. Membrane characterization

2.3.1. SEM and EDAX

The surface and cross-sectional morphologies of the membranes were investigated using scanning electron microscopy (SEM). The prepared membranes were fractured in liquid nitrogen and coated with gold before SEM analysis. SEM device was equipped with dispersive X-ray analysis (EDAX) detector to inspect dispersion of nano-ZnO particles in the cross-section of the fabricated membranes. SEM images were taken under very high-vacuum conditions, operating at 20 kV.

Table 1The compositions of the fabricated membranes.

Membrane	PVC (wt%)	PEG 6 kDa (wt%)	ZnO (wt%)	NMP (wt%)
Unmodified EPVC	15.0	4.0	0.0	81.0
0.3 wt% ZnO/PVC	15.0	4.0	0.3	80.7
1 wt%	15.0	4.0	1.0	80.0
2 wt%	15.0	4.0	2.0	79.0
3 wt%	15.0	4.0	3.0	78.0
4 wt%	15.0	4.0	4.0	77.0

2.3.2. Pore size and porosity

The average porosity of the fabricated membranes was measured by the gravimetric method, as indicated below [34]:

$$p = \frac{\omega_1 - \omega_2}{A \times l \times d_w} \tag{1}$$

where ω_1 and ω_2 are the weight of the wet and dry membrane, respectively. A is the membrane area (m²), l is the membrane thickness (m) and d_w is the water density (0.998 g/cm³). For porosity measurement, at first pieces of membrane with specific area were immersed in distillated water at least for 12 h to ensure that all the pores of the membranes were filled. Immediately after that water on the surface of the samples were cleaned cautiously and they were weighted. Subsequently, the samples were put in oven for 2 h at 60 °C to evaporate water from membrane pores and weighted again.

Guerout–Elford–Ferry relation (Eq. (2)), was used to measure mean pore radius (r_m) of the membranes [34]:

$$r_{m} = \sqrt{\frac{(2.9-1.75p)\times 8\eta lQ}{p\times A\times \Delta P}} \eqno(2)$$

where Q is water flux (m³/s), η is the water viscosity (8.9 × 10⁻⁴ Pa s) and ΔP is the operation pressure (0.2 MPa).

2.3.3. Contact angle

Deionized water was used as a probe liquid to specify the changes in the hydrophobicity of the membrane surface. The results were obtained using OCA20, Dataphysics Instruments, Germany, which were taken at 25 °C. A deionized water droplet was placed on the surface of the membranes, and then the contact angle between the water and the membrane was measured until no change was observed. At least, five measurements were taken at different locations on the membrane surface to determine the average contact angle value.

2.4. Performance experiments

2.4.1. Ultrafiltration test apparatus

UF tests were done by an apparatus that was explained in our previous paper [8]. Briefly, water and BSA flux through the membranes were measured by a dead-end cell which had an effective area about 20 cm². The feed (pure water or BSA) enters the cell from the tank above it, and N₂ pressure provides the needed driving force for the feed to permeate through the membranes. Moreover, as the feed in the cell was continuously stirred by a magnetic stirrer, concentration of the feed in cell can be considered homogenous. The permeation through the membranes was weighted by a balance every 10 min and a computer records this data for further analysis. Fig. 1 shows the applied dead-end setup.

2.4.2. Calculation of permeation, flux recovery and BSA rejection

Water and BSA flux measurements were carried out at operating pressure of 2 bar and BSA concentration was 500 ppm. First, the setup was allowed to work with higher pressure (3 bar) for 30 min. Then, for 90 min pure water flux was calculated as follows:



Fig. 1. Dead-end setup for testing performance of the membranes.

$$J = \frac{M}{A\Delta t} \tag{3}$$

where J, M, A and Δt were flux, the mass of permeated water, membrane effective area and permeation time.

After water flux calculation, in order to analyze antifouling properties of the membranes, the feed tank was filled with 500 ppm BSA solution and BSA permeation was obtained. BSA flux test was done for 90 min. After that, before filling the feed tank with distillated water to calculate second water flux after BSA, the membranes were put in fresh water for 1 h for washing.

Finally, the flux recovery ratio (FRR) was measured with having the first and second water flux. as follows:

$$FRR \ (\%) = \left(\frac{J_{water,1}}{J_{water,2}}\right) \times 100 \tag{4}$$

where $J_{water,1}$ and $J_{water,2}$ were flux of pure water after and before BSA flux, respectively.

The percentage of BSA rejection (*R*) was another factor to evaluate membranes' performance and was calculated using the following equation:

$$R (\%) = \left(1 - \frac{C_p}{C_f}\right) \times 100 \tag{5}$$

where C_p and C_f are BSA concentration in permeate and feed, respectively.

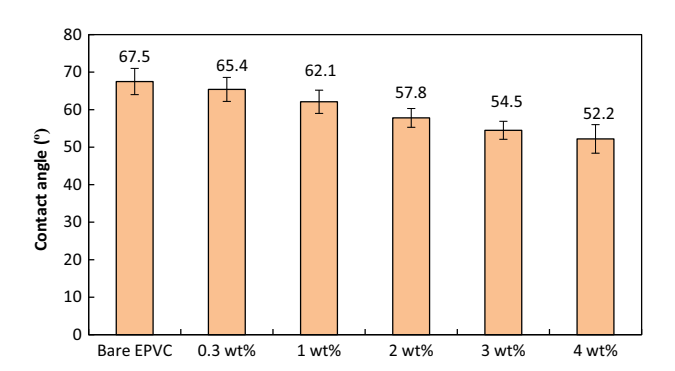


Fig. 2. Static water contact angle of the bare and the nanocomposite membranes.

3. Results and discussion

3.1. Characterization of the nanocomposite membranes

Contact angle test was applied at 25 °C to study changes in surface hydrophilicity of the membranes, as shown in Fig. 2. As it is obvious, contact angle decreases continuously with increasing ZnO loading. It is due to increment of ZnO presence in the surface

(a) Bare EPVC

of the membranes. Thereby, the membranes become more hydrophilic after ZnO addition, and they will have more water flux with better antifouling properties [47].

SEM images and EDAX analysis were utilized to investigate changes in cross-section and surface morphology of the mixed matrix membranes after ZnO addition and the results are presented in Figs. 3–6. The cross-section images are shown in Fig. 3, and as it can be seen, all the membranes have typical asymmetric,

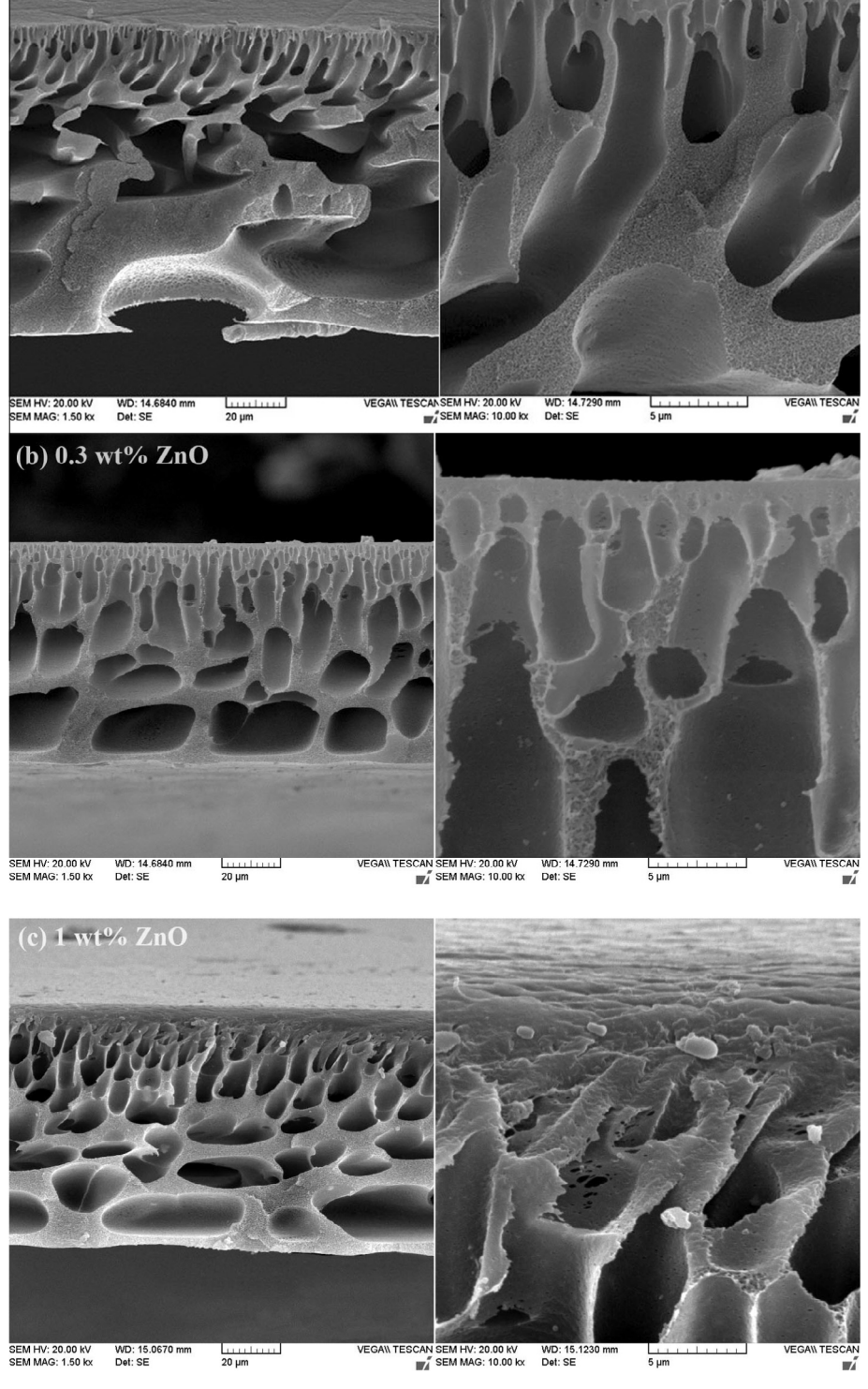


Fig. 3. Cross-sectional SEM images of the bare PVC and the ZnO/PVC nanocomposite membranes at two magnifications.

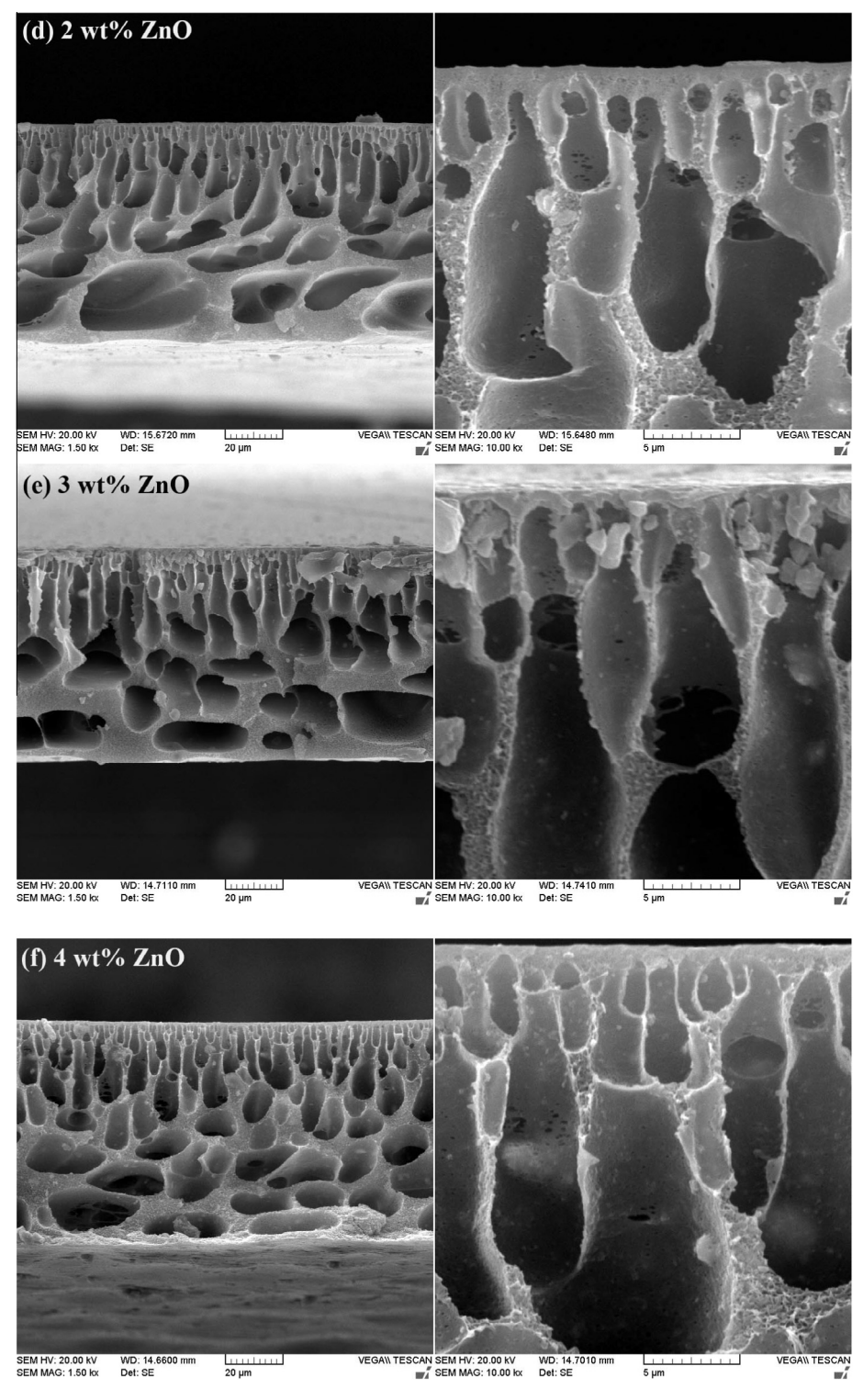


Fig. 3 (continued)

highly porous and inhomogeneous morphology with a dense top layer which is responsible for permeation and rejection [44]. Morphologies of the asymmetric membranes fabricated via phase inversion are highly influenced by thermodynamic and kinetic of the system and ZnO addition affects these two factors. For the bare PVC ultrafiltration membranes because of high affinity between solvent (NMP) and nonsolvent (water), membrane cross section has large and finger-like pores. This affinity between NMP and water increases the rate of NMP-water exchange in the process

of membrane formation and leads to faster instantaneous demixing; consequently, membranes with high porosity are formed [12,48].

With ZnO addition, the amount of pores in the hybrid membranes increases and for ZnO/PVC membranes, seems that porosity is on the growth as ZnO content increases. In addition, the connectivity between top-layer and the bottom improves with ZnO addition. Also, the macro-void volume of all the ZnO/PES hybrid membranes appears to be greater than the bare PVC membrane,

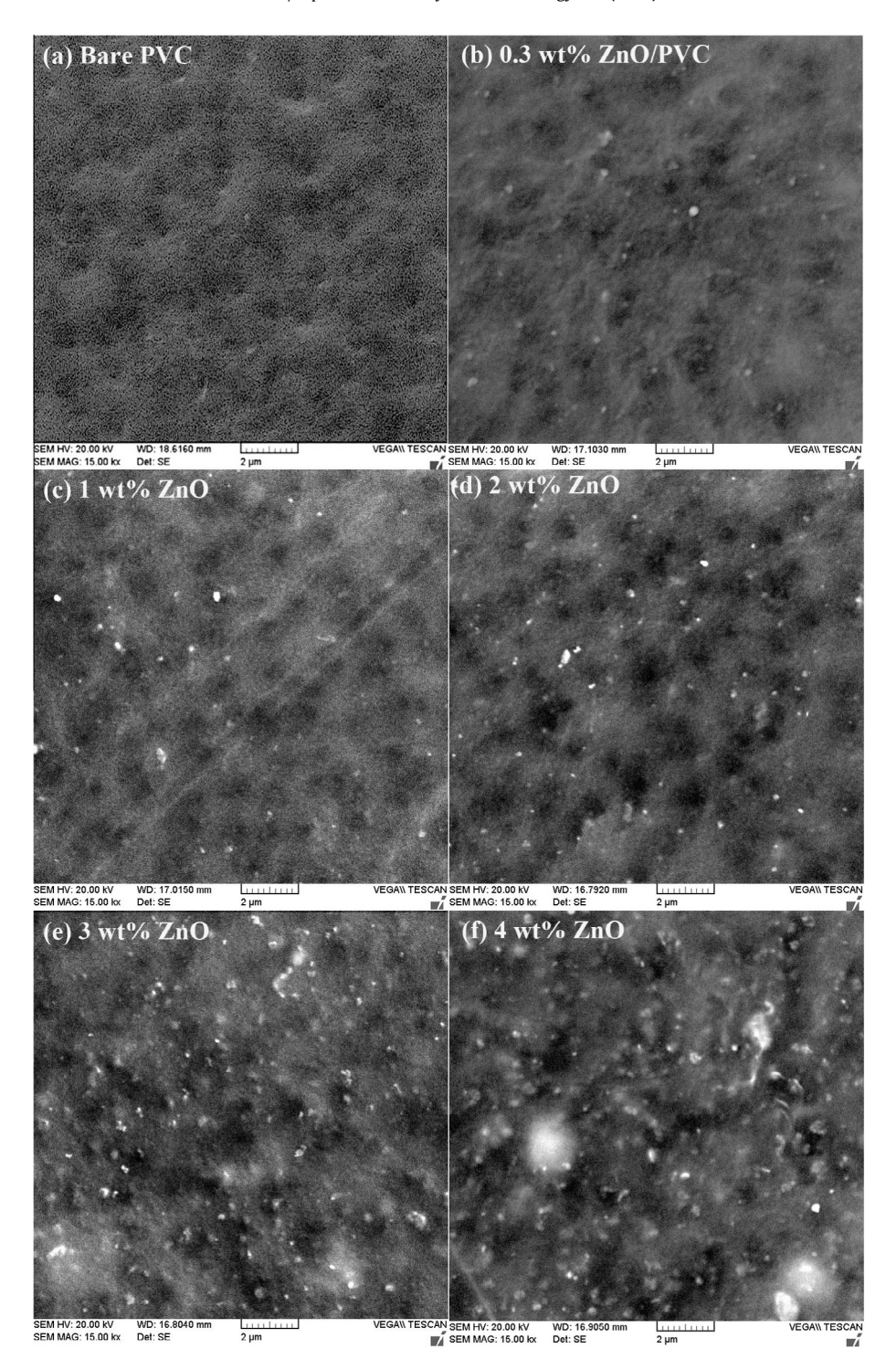
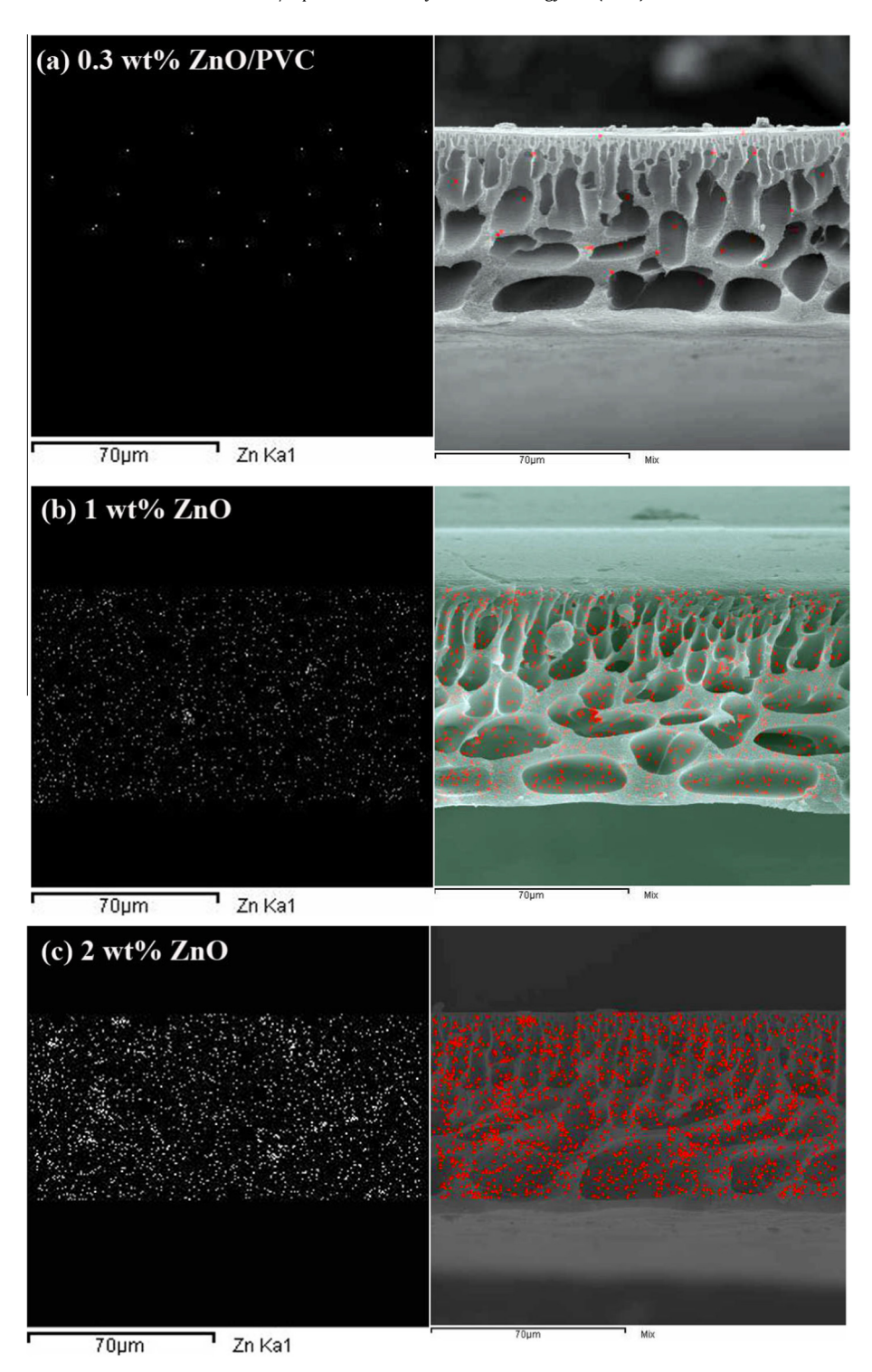


Fig. 4. Surface SEM images of the bare PVC and the ZnO/PVC nanocomposite membranes.

in particular up to 3 wt% ZnO and after that it reduces. This observation is in accordance with the data of porosity, which is presented in Table 2. However, for the case of 4 wt% ZnO/PVC membrane the volume of pores of the membrane is obviously lower than that for 3 wt% ZnO/PVC membrane, which means that after 3 wt% ZnO addition the desired morphology disappeared. The reason for this phenomenon is higher chance of aggregation for ZnO nanoparticles at high loading, which it can be seen in surface SEM images (Fig. 4f). In addition, as ZnO loading increases, the viscosity of polymeric solution goes up and although the viscosities were not measured precisely in this study, increment in viscosity

of the polymeric suspension with ZnO addition was visually observed, and also this has been reported at similar papers [34,49,50]. These observations are consistent with other similar studies about nanocomposite membranes [42]. Improvement in pores connectivity across the membranes and porosity have considerable effect on water flux, which will be discussed later.

The SEM images were also used to visualize changes in surface morphology after ZnO addition and the images are shown in Fig. 4. As it can be seen, as ZnO was added to the membrane structure, more nanoparticles were agglomerated in the surface of the membranes. This observation can be clearly seen from the EDAX



 $\textbf{Fig. 5.} \ \ \textbf{EDAX} \ \ \textbf{of cross section of the ZnO/PVC nanocomposite membranes}.$

analysis of Zn element, depicted in Fig. 6. The EDAX is an appropriate method to study particles dispersion in membrane and also shows how with addition of more nanoparticles, they move more toward the surface of membrane and have a tendency to make cluster [42,51]. Based on Fig. 6, ZnO agglomeration in surface for membranes with 4 wt% ZnO is quite visible. This agglomeration of the nanoparticles at the surface can lead to pore blockage and consequently, membrane water flux is expected to reduce for this membrane [8].

This nanoparticle agglomeration can be also seen in the cross-section, as it is shown in Fig. 5. At low ZnO concentrations, the nanofillers are homogeneously dispersed and particle aggregation is negligible. As ZnO increases to 3 wt%, low agglomeration can be observed, however, at higher loading this phenomenon is clear. EDAX analysis is also useful to investigate and compare the amount of added nanoparticles in polymeric solution with the prepared and dried membranes. The results of this section show that ZnO nanoparticles in the prepared membranes are 0.29 ± 0.02 ,

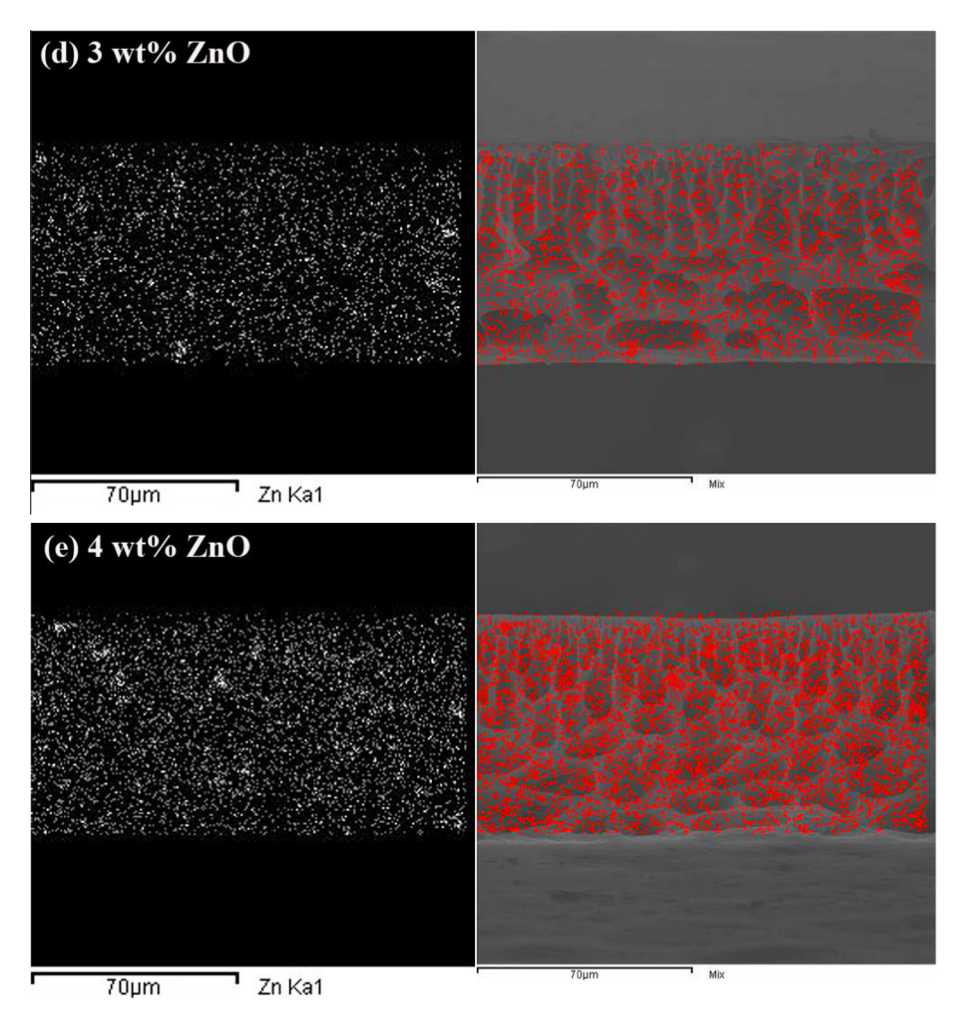


Fig. 5 (continued)

 0.95 ± 0.09 , 1.91 ± 0.19 , 2.89 ± 0.24 and 3.92 ± 0.28 for 0.3, 1, 2, 3 and 4 wt% ZnO/PVC membranes, respectively. These results confirm that nanoparticle leaching during membrane formation is negligible.

3.2. Filtration properties

3.2.1. Permeation and rejection results

Pure water and BSA flux of the prepared membranes were measured at operating pressure of 2 bar. As it is shown in Fig. 7, the pure water flux increases continuously with addition of ZnO nanoparticles up to 3 wt%, then it decreases. Increment in water flux is indeed due to higher surface hydrophilicity of the membranes (Fig. 2) and also, more porous structure of the membranes (see Table 2) [43,50,52]. However, as the amount of the nanoparticle reaches 4 wt%, they are more likely to aggregate and causing pore blockage at membrane surface (see Fig. 4), therefore permeation reduces [42]. This feature was observed in EDAX analysis and agglomeration of the nanoparticles at high loading was almost noticeable. When membranes surface become hydrophilic (as seen in Fig. 2), they attract water molecules easier, which means water permeation occurs faster [33]. Plus, as the membranes become more porous with higher interconnectivity in the structure of the membranes, resistance to water permeation reduce, consequently, the flux increases. Membranes mean pore size also increases after ZnO addition (Table 2), which indicates water penetration, and flux takes place easier. These reasons were concluded from membrane characterization results.

However, ZnO addition causes changes in both prepared membranes and polymeric solution, which can neutralize the effect of flux-increasing factors. First, as mentioned earlier, ZnO addition leads to more viscous polymeric solution [34,49,50], and as the viscosity increases, it leads delay in instantaneous demixing and solvent-non solvent exchange rate; thereby membranes with denser structure are formed [45]. It was found out by measuring membranes' porosity and mean pore size, which are presented in Table 2 and reduction in both parameters at high nanoparticle contents was observed. Although all the fabricated membranes have porosity above 68%, which is mainly because of existence of PEG in polymeric solution and acting as a pore former during membrane formation [7,53], ZnO addition even leads to more porous membranes. This is indeed due to positive effect of ZnO addition in having instantaneous demixing and faster water-NMP diffusion; however, as discussed above, at 4 wt% ZnO content, porosity declines [8]. The same trend was also seen for the case of mean pore size because of the same reason [44].

First, according to Fig. 3f, it is obvious that the pores of membranes become less connected for this ZnO content. Thereby, water penetration becomes harder. Second, the nanoparticles aggregation at 4 wt% loading seems inevitable. All the polymeric solutions in this study were sonicated for several hours to eliminate the possibility of this phenomenon, but as observed in EDAX analysis, at this ZnO concentration, it happens and causes pore blockage at

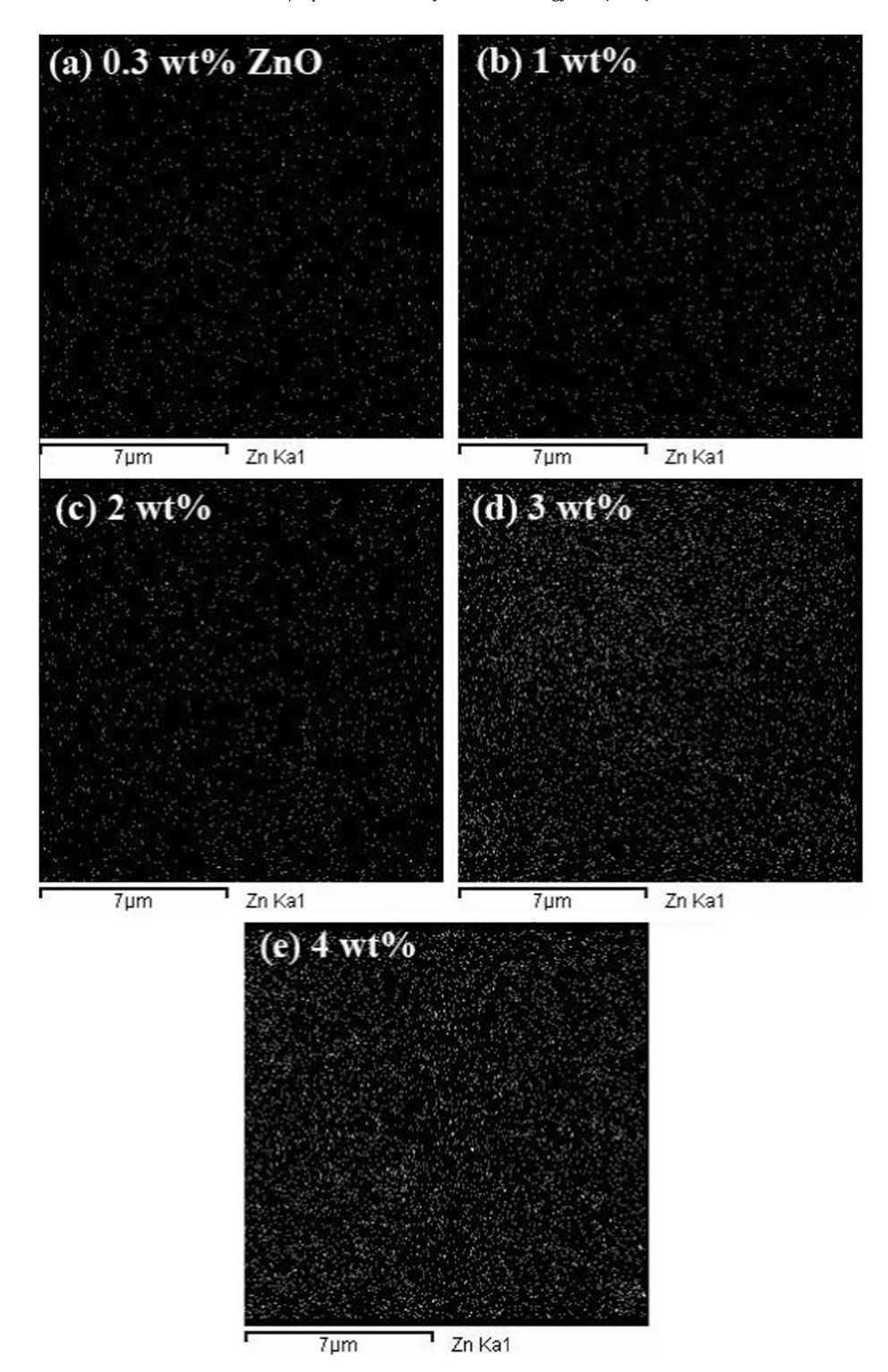


Fig. 6. Surface EDAX of the ZnO/PVC nanocomposite membranes.

Table 2Mean pore size and porosity of the prepared membranes.

Membrane	Mean pore size (nm)	Average porosity (%)	
Unmodified EPVC	9.3 (±0.4)	67.9 (±2.9)	
0.3 wt% ZnO/PVC	9.8 (±0.5)	70.5 (±3.5)	
1 wt%	10.5 (±0.5)	75.1 (±3.3)	
2 wt%	11.2 (±0.6)	77.3 (±3.9)	
3 wt%	12.1 (±0.8)	79.8 (±4.1)	
4 wt%	11.5 (±0.7)	76.2 (±3.8)	

the surface. Therefore, the flux though UF nanocomposite membranes are a trade-off between the above-mentioned parameters and reasons and similar results are reported in literature [33,42,54].

In addition to high water flux, the modified UF membranes should be able to reject BSA at high percentages. Based on the BSA rejection results, shown in Fig. 8, all the membranes reject BSA more than 90% and ZnO addition leads to even better BSA rejection (above 97%) [31]. BSA, which is used as a foulant in this study, has more affinity with more hydrophobic materials and

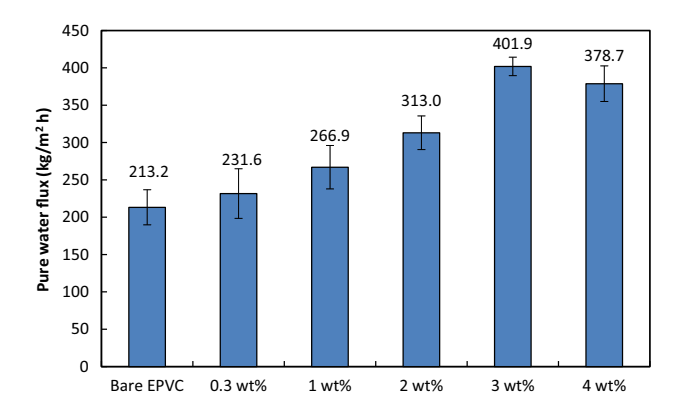


Fig. 7. Pure water flux through the unmodified and the ZnO-modified PVC UF membranes.

can be attracted by them. Hence, the increment in BSA rejection can be justified because of more hydrophilic surface after ZnO addition. Slight changing in this trend after 4 wt% ZnO addition is related to the nanoparticles aggregation, which blocks surface pores, in particular, smaller pores, therefore, more large pores are active and this leads to reduction in BSA rejection [8,33,55].

3.2.2. Antifouling ability of the membranes

One of the most important factors that should be improved for filtration membranes is antifouling characteristic. Especially, this issue is more serious for hydrophobic materials like PVC and PVDF. Fouling means that some components (like proteins, whey or micro-organism) have a tendency to adsorb on or in the surface of pores; thereby they affect water flux over time. That is why in many industrial processes where membranes are used for water purification, membranes should be washed after a particular time to recover their separation capacity [56]. However, the fouling is not always reversible and removable through washing, and this makes modification of the membranes to prepare membranes for anti-reversible fouling more required [44,57]. For investigation this ability, water flux of the membranes should be calculated after they have been in contact with foulant agents. Therefore, water flux before and after being in contact with BSA has been measured and compared, and the results are shown in Fig. 9. Permeation results indicate that in all the steps, they follow a similar trend. They usually start with higher flux and after a while; they become steady. Pure water flux is much more than flux of feed containing 500 ppm BSA, thereby membranes are more permeable for water than BSA.

However, as BSA passes through the membranes, it can interact with internal surface and form a layer on them. This will result in

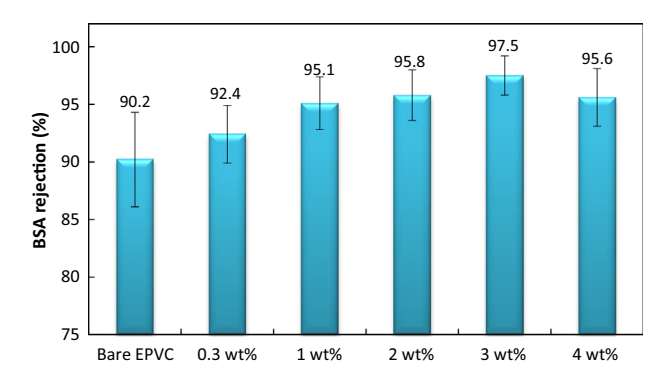


Fig. 8. BSA rejection from the unmodified and the ZnO-modified PVC UF membranes.

lower flux due to increased resistance. Therefore, in order to improve antifouling ability of the membranes, their surface should be less to attract BSA. Addition of hydrophilic nanoparticles results in a less hydrophobic surface, as a result antifouling enhances [47,51,58].

The FRR data (Fig. 10) shows that incorporation of ZnO nanoparticles results in much better antifouling properties of PVC membranes. Unmodified EPVC membranes are able to recover 69% of their pure water flux after BSA permeation, which for the membranes containing 3 wt% ZnO, this number rises to around 92%, thereby antifouling of PVC membranes has been quite improved. Similar results are also reported in other nanocomposite membranes [8,43,44,59].

The comparison of pure water flux, BSA flux and *FRR* in this work with our previous study about PVC/TiO₂ UF membranes [8] at the optimized nanoparticle addition (2 wt% for TiO₂ and 3 wt% for ZnO) shows that although that PVC/TiO₂ had more water flux, the recovery ratio and BSA flux for PVC/ZnO is higher. It is probably due to higher hydrophilicity of the 3 wt% ZnO/PVC related to 2 wt% TiO₂/PVC membrane. The contact angle of 3 wt% ZnO/PVC is 54.5°, whereas this is 57.2° [8] for 2 wt% TiO₂/PVC membrane. High hydrophilicity decreases the protein attachment to the membrane surface and therefore, the flux reduction of 3 wt% ZnO/PVC is lower than 2 wt% TiO₂/PVC membrane. Consequently, as it is shown in Fig. 11, PVC/ZnO seems to be less susceptible to fouling, and they are more suitable where fouling is a serious issue.

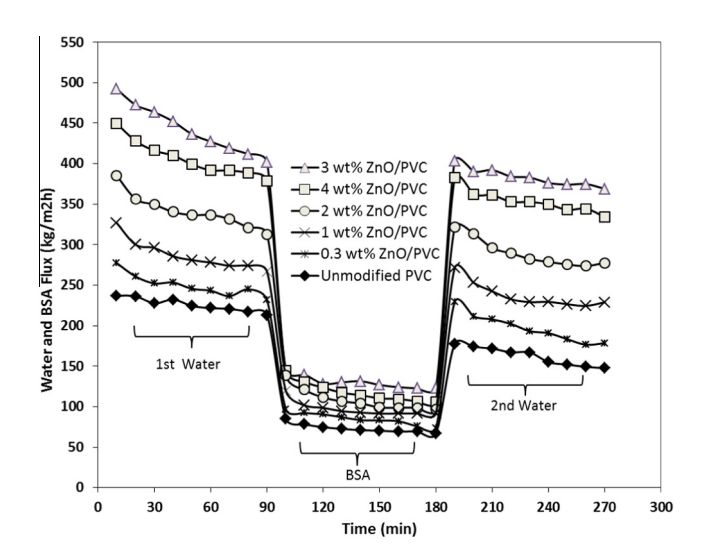


Fig. 9. Flux of water and BSA in three 90 min sections: first for pure water, second for BSA and third for pure water after washing the membranes for 30 min.

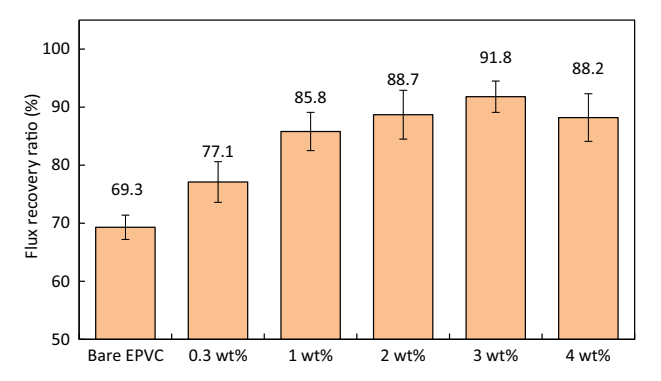


Fig. 10. Flux recovery ratio of the prepared membranes.

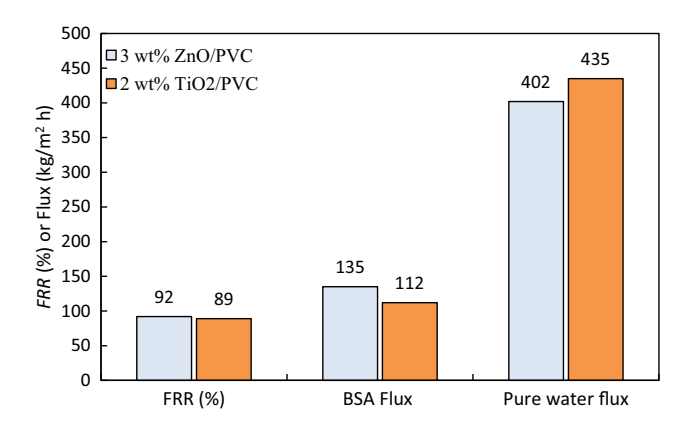


Fig. 11. Comparison between PVC/ZnO and PVC/TiO $_2$ UF membranes.

4. Conclusions

ZnO nanoparticles were chosen to modify morphology and performance of PVC UF membranes. ZnO at five different percentages from 0.3 wt% to 4 wt% was added to the polymeric casting solution, including PEG 6 kDa as a pore former and NMP as a solvent. The membranes were fabricated via the phase inversion method. The SEM images indicated remarkable changes in the membranes' structure and higher connectivity among channels with ZnO addition up to 3 wt%. Also, EDAX analyses showed fine dispersion of the nanoparticles in the membranes' structure. ZnO led to increase in water flux of the membranes from 213 kg/m²h for the bare PVC membrane to 402 kg/m²h for 3 wt% ZnO/PVC membrane, mainly because of higher surface hydrophilicity of the modified membranes and more porous structure. However, with more ZnO addition permeation declined, which is due to the nanoparticles' agglomeration and denser morphology at this ZnO content. Flux recovery ratio improved with ZnO addition, and the membranes showed much better antifouling properties in comparison with the bare membrane. The results showed that addition of 3 wt% ZnO was optimum to obtain the best results for water flux. flux recovery and BSA rejection and more ZnO addition caused a reduction in these parameters.

References

- A. Brunetti, F. Scura, G. Barbieri, E. Drioli, Membrane technologies for CO₂ separation, J. Membr. Sci. 359 (2010) 115–125.
- [2] A. Arunkumar, M.R. Etzel, Negatively charged tangential flow ultrafiltration membranes for whey protein concentration, J. Membr. Sci. 475 (2015) 340– 348.
- [3] A.L. Ahmad, M. Sarif, S. Ismail, Development of an integrally skinned ultrafiltration membrane for wastewater treatment: effect of different formulations of PSf/NMP/PVP on flux and rejection, Desalination 179 (2005) 257–263.
- [4] S. Alzahrani, A.W. Mohammad, Challenges and trends in membrane technology implementation for produced water treatment: a review, J. Water Proc. Eng. 4 (2014) 107–133.
- [5] R. Salcedo-Diaz, R. Ruiz-Femenia, J.A. Caballero, Optimal design of a hybrid membrane system combining reverse and forward osmosis for seawater desalination, in: P.S.V. Jiří Jaromír Klemeš, L. Peng Yen (Eds.), Computer Aided Chemical Engineering, Elsevier, 2014, pp. 1399–1404.
 [6] K. Lutchmiah, A.R.D. Verliefde, K. Roest, L.C. Rietveld, E.R. Cornelissen, Forward
- [6] K. Lutchmiah, A.R.D. Verliefde, K. Roest, L.C. Rietveld, E.R. Cornelissen, Forward osmosis for application in wastewater treatment: a review, Water Res. 58 (2014) 179–197.
- [7] M.H.D.A. Farahani, H. Rabiee, V. Vatanpour, S.M. Borghei, Fouling reduction of emulsion polyvinylchloride ultrafiltration membranes blended by PEG: the effect of additive concentration and coagulation bath temperature, Des. Water Treat. (2015) 1–14, http://dx.doi.org/10.1080/19443994.2015.1048739.
- [8] H. Rabiee, M.H.D.A. Farahani, V. Vatanpour, Preparation and characterization of emulsion polyvinyl chloride (EPVC)/TiO₂ nanocomposite ultrafiltration membrane, J. Membr. Sci. 472 (2014) 185–193.
- [9] S. Mehdipour, V. Vatanpour, H.-R. Kariminia, Influence of ion interaction on lead removal by a polyamide nanofiltration membrane, Desalination 362 (2015) 84–92.

- [10] M. Kraume, A. Drews, Membrane bioreactors in waste water treatment–status and trends, Chem. Eng. Technol. 33 (2010) 1251–1259.
- [11] H. Strathmann, K. Kock, P. Amar, The formation mechanism of asymmetric membranes, Desalination 16 (1975) 179–203.
- [12] S.K. Yong, J.K. Hyo, Y.K. Un, Asymmetric membrane formation via immersion precipitation method. I. Kinetic effect, J. Membr. Sci. 60 (1987) 219–232.
- [13] M. Safarpour, A. Khataee, V. Vatanpour, Preparation of a novel polyvinylidene fluoride (PVDF) ultrafiltration membrane modified with reduced graphene oxide/titanium dioxide (TiO₂) nanocomposite with enhanced hydrophilicity and antifouling properties, Ind. Eng. Chem. Res. 53 (2014) 13370–13382.
- [14] B. Chakrabarty, A.K. Ghoshal, M.K. Purkait, Preparation, characterization and performance studies of polysulfone membranes using PVP as an additive, J. Membr. Sci. 315 (2008) 36–47.
- [15] A. Idris, N. Mat Zain, M.Y. Noordin, Synthesis, characterization and performance of asymmetric polyethersulfone (PES) ultrafiltration membranes with polyethylene glycol of different molecular weights as additives, Desalination 207 (2007) 324–339.
- [16] E. Saljoughi, T. Mohammadi, Cellulose acetate (CA)/polyvinylpyrrolidone (PVP) blend asymmetric membranes: preparation, morphology and performance, Desalination 249 (2009) 850–854.
- [17] N. Scharnagl, H. Buschatz, Polyacrylonitrile (PAN) membranes for ultra- and microfiltration, Desalination 139 (2001) 191–198.
- [18] S. Yang, Z. Liu, Preparation and characterization of polyacrylonitrile ultrafiltration membranes, J. Membr. Sci. 222 (2003) 87–98.
- [19] X. Fan, Y. Su, X. Zhao, Y. Li, R. Zhang, J. Zhao, Z. Jiang, J. Zhu, Y. Ma, Y. Liu, Fabrication of polyvinyl chloride ultrafiltration membranes with stable antifouling property by exploring the pore formation and surface modification capabilities of polyvinyl formal, J. Membr. Sci. 464 (2014) 100– 109.
- [20] W. Albrecht, T. Weigel, M. Schossig-Tiedemann, K. Kneifel, K.V. Peinemann, D. Paul, Formation of hollow fiber membranes from poly(ether imide) at wet phase inversion using binary mixtures of solvents for the preparation of the dope, J. Membr. Sci. 192 (2001) 217–230.
- [21] J. Liu, Y. Su, J. Peng, X. Zhao, Y. Zhang, Y. Dong, Z. Jiang, Preparation and performance of antifouling PVC/CPVC blend ultrafiltration membranes, Ind. Eng. Chem. Res. 51 (2012) 8308–8314.
- [22] B. Liu, C. Chen, W. Zhang, J. Crittenden, Y. Chen, Low-cost antifouling PVC ultrafiltration membrane fabrication with Pluronic F 127: effect of additives on properties and performance, Desalination 307 (2012) 26–33.
- [23] W. Shu, C.F. Xiao, X.Y. Hu, S. Mei, Preparation of hydrophilic and antifouling PVC/PAN hollow fiber membrane, Adv. Mater. Res. 332–334 (2011) 1764– 1768
- [24] Q.F. An, J.W. Qian, H.B. Sun, L.N. Wang, L. Zhang, H.L. Chen, Compatibility of PVC/EVA blends and the pervaporation of their blend membranes for benzene/cyclohexane mixtures, J. Membr. Sci. 222 (2003) 113–122.
- [25] M. Bodzek, K. Konieczny, The influence of molecular mass of poly (vinyl chloride) on the structure and transport characteristics of ultrafiltration membranes, J. Membr. Sci. 61 (1991) 131–156.
- [26] S. Mei, C. Xiao, X. Hu, Preparation of porous PVC membrane via a phase inversion method from PVC/DMAc/water/additives, J. Appl. Polym. Sci. 120 (2011) 557–562.
- [27] X. Shi, G. Tal, N.P. Hankins, V. Gitis, Fouling and cleaning of ultrafiltration membranes: a review, J. Water Process Eng. 1 (2014) 121–138.
- [28] A.V.R. Reddy, H.R. Patel, Chemically treated polyethersulfone/polyacrylonitrile blend ultrafiltration membranes for better fouling resistance, Desalination 221 (2008) 318–323.
- [29] Y. Xiuli, C. Hongbin, W. Xiu, Y. Yongxin, Morphology and properties of hollowfiber membrane made by PAN mixing with small amount of PVDF, J. Membr. Sci. 146 (1998) 179–184.
- [30] M. Amirilargani, A. Sabetghadam, T. Mohammadi, Polyethersulfone/ polyacrylonitrile blend ultrafiltration membranes with different molecular weight of polyethylene glycol: preparation, morphology and antifouling properties, Polym. Adv. Technol. 23 (2012) 398–407.
- [31] N. Maximous, G. Nakhla, W. Wan, K. Wong, Preparation, characterization and performance of Al₂O₃/PES membrane for wastewater filtration, J. Membr. Sci. 341 (2009) 67–75.
- [32] X. Liu, Y. Peng, S. Ji, A new method to prepare organic-inorganic hybrid membranes, Desalination 221 (2008) 376–382.
- [33] V. Vatanpour, S.S. Madaeni, A.R. Khataee, E. Salehi, S. Zinadini, H.A. Monfared, TiO₂ embedded mixed matrix PES nanocomposite membranes: influence of different sizes and types of nanoparticles on antifouling and performance, Desalination 292 (2012) 19–29.
- [34] J.-F. Li, Z.-L. Xu, H. Yang, L.-Y. Yu, M. Liu, Effect of TiO₂ nanoparticles on the surface morphology and performance of microporous PES membrane, Appl. Surf. Sci. 255 (2009) 4725–4732.
- [35] G. Wu, S. Gan, L. Cui, Y. Xu, Preparation and characterization of PES/TiO₂ composite membranes, Appl. Surf. Sci. 254 (2008) 7080–7086.
- [36] V. Vatanpour, S.S. Madaeni, L. Rajabi, S. Zinadini, A.A. Derakhshan, Boehmite nanoparticles as a new nanofiller for preparation of antifouling mixed matrix membranes, J. Membr. Sci. 401–402 (2012) 132–143.
- [37] S. Zinadini, A.A. Zinatizadeh, M. Rahimi, V. Vatanpour, H. Zangeneh, Preparation of a novel antifouling mixed matrix PES membrane by embedding graphene oxide nanoplates, J. Membr. Sci. 453 (2014) 292–301.
- [38] V. Vatanpour, S.S. Madaeni, R. Moradian, S. Zinadini, B. Astinchap, Novel antibifouling nanofiltration polyethersulfone membrane fabricated from

- embedding TiO_2 coated multiwalled carbon nanotubes, Sep. Purif. Technol. 90 (2012) 69–82.
- [39] V. Vatanpour, M. Esmaeili, M.H.D.A. Farahani, Fouling reduction and retention increment of polyethersulfone nanofiltration membranes embedded by amine-functionalized multi-walled carbon nanotubes, J. Membr. Sci. 466 (2014) 70–81.
- [40] N. Maximous, G. Nakhla, W. Wan, K. Wong, Performance of a novel ZrO₂/PES membrane for wastewater filtration, J. Membr. Sci. 352 (2010) 222–230.
- [41] Z. Dong, W. Jing, W. Xing, Triblock polymer template assisted sol–gel process for fabrication of multi-channel TiO₂/ZrO₂ ultrafiltration membrane, J. Membr. Sci. 373 (2011) 167–172.
- [42] L. Shen, X. Bian, X. Lu, L. Shi, Z. Liu, L. Chen, Z. Hou, K. Fan, Preparation and characterization of ZnO/polyethersulfone (PES) hybrid membranes, Desalination 293 (2012) 21–29.
- [43] C.P. Leo, W.P. Cathie Lee, A.L. Ahmad, A.W. Mohammad, Polysulfone membranes blended with ZnO nanoparticles for reducing fouling by oleic acid, Sep. Purif. Technol. 89 (2012) 51–56.
- [44] S. Liang, K. Xiao, Y. Mo, X. Huang, A novel ZnO nanoparticle blended polyvinylidene fluoride membrane for anti-irreversible fouling, J. Membr. Sci. 394–395 (2012) 184–192.
- [45] S. Zhao, W. Yan, M. Shi, Z. Wang, J. Wang, S. Wang, Improving permeability and antifouling performance of polyethersulfone ultrafiltration membrane by incorporation of ZnO-DMF dispersion containing nano-ZnO and polyvinylpyrrolidone, J. Membr. Sci. 478 (2015) 105–116.
- [46] N. Maximous, G. Nakhla, K. Wong, W. Wan, Optimization of Al₂O₃/PES membranes for wastewater filtration, Sep. Purif. Technol. 73 (2010) 294–301.
- [47] E. Yuliwati, A.F. Ismail, Effect of additives concentration on the surface properties and performance of PVDF ultrafiltration membranes for refinery produced wastewater treatment, Desalination 273 (2011) 226–234.
- [48] Q.-Z. Zheng, P. Wang, Y.-N. Yang, D.-J. Cui, The relationship between porosity and kinetics parameter of membrane formation in PSF ultrafiltration membrane, J. Membr. Sci. 286 (2006) 7–11.

- [49] Y. Yang, P. Wang, Q. Zheng, Preparation and properties of polysulfone/TiO₂ composite ultrafiltration membranes, J. Polym. Sci., Part B: Polym. Phys. 44 (2006) 879–887.
- [50] Y. Yang, H. Zhang, P. Wang, Q. Zheng, J. Li, The influence of nano-sized TiO₂ fillers on the morphologies and properties of PSF UF membrane, J. Membr. Sci. 288 (2007) 231–238.
- [51] S.J. Oh, N. Kim, Y.T. Lee, Preparation and characterization of PVDF/TiO₂ organic-inorganic composite membranes for fouling resistance improvement, J. Membr. Sci. 345 (2009) 13–20.
- [52] X. Cao, J. Ma, X. Shi, Z. Ren, Effect of TiO₂ nanoparticle size on the performance of PVDF membrane, Appl. Surf. Sci. 253 (2006) 2003–2010.
- [53] M. Amirilargani, E. Saljoughi, T. Mohammadi, Improvement of permeation performance of polyethersulfone (PES) ultrafiltration membranes via addition of Tween-20, J. Appl. Polym. Sci. 115 (2010) 504–513.
- [54] J.-N. Shen, H.-M. Ruan, L.-G. Wu, C.-J. Gao, Preparation and characterization of PES-SiO₂ organic-inorganic composite ultrafiltration membrane for raw water pretreatment, Chem. Eng. J. 168 (2011) 1272–1278.
- [55] N.A.A. Hamid, A.F. Ismail, T. Matsuura, A.W. Zularisam, W.J. Lau, E. Yuliwati, M. S. Abdullah, Morphological and separation performance study of polysulfone/titanium dioxide (PSF/TiO2) ultrafiltration membranes for humic acid removal, Desalination 273 (2011) 85–92.
- [56] M. Padaki, D. Emadzadeh, T. Masturra, A.F. Ismail, Antifouling properties of novel PSf and TNT composite membrane and study of effect of the flow direction on membrane washing, Desalination 362 (2015) 141–150.
- [57] D. Rana, T. Matsuura, Surface modifications for antifouling membranes, Chem. Rev. 110 (2010) 2448–2471.
- [58] A. Alpatova, E.-S. Kim, X. Sun, G. Hwang, Y. Liu, M. Gamal El-Din, Fabrication of porous polymeric nanocomposite membranes with enhanced anti-fouling properties: effect of casting composition, J. Membr. Sci. 444 (2013) 449–460.
- [59] S.S. Madaeni, S. Zinadini, V. Vatanpour, A new approach to improve antifouling property of PVDF membrane using in situ polymerization of PAA functionalized TiO₂ nanoparticles, J. Membr. Sci. 380 (2011) 155–162.